Egypt.J.Chem. **Vol. 63**, No.7. pp. 2631 - 2646 (2020)

Egyptian Journal of Chemistry
http://ejchem.journals.ekb.eg/

Chenopodium Murale Essential Oil Alleviates The Genotoxicity and Oxidative Stress of Silver Nanoparticles in The Rat Kidney

Mosaad A. Abdel-Wahhab[1*], Helmy M.S. Ahmed[2], Aziza A. El-Nekeety[1], Sekena H. Abdel-Aziem[3], Hafiza A. Sharaf[4], Mohamed S. Abdel-Aziz[5], Mohamed F. Sallam[6], Fathia A. Mannaa[7]

[1]*Food Toxicology & Contaminants Dept., National Research Center, Dokki, Cairo, Egypt.*
[2]*Toxicology & Pharmacology Dept., Faculty of Pharmacy, Cairo University, Cairo, Egypt.*
[3]*Cell Biology Dept. National Research Center, Dokki, Cairo, Egypt.*
[4]*Pathology Dept., National Research Center, Dokki, Cairo, Egypt.*
[5]*Microbial Chemistry Dept., National Research Center, Dokki, Cairo, Egypt.*
[6]*New Kasr Al-Ainy Hospital, Cairo, Egypt.*
[7]*Physiology Dept. National Research Center, Dokki, Cairo, Egypt.*

THIS study aimed to synthesize silver nanoparticles (AgNPs) using *Chenopodium murale* extract (CME), to evaluate the antioxidant activity of the *Chenopodium murale* essential oil (CMEO) and the protective role against nephrotoxicity of AgNPs. Seven groups of female Sprague-Dawley rats were treated orally for 21 days included the control group, AgNPs-treated groups (25 or 50 mg/kg b.w), CMEO-treated groups (0.5 or 1 mg/kg b.w) and AgNPs plus CMEO-treated groups. The synthesized AgNPs were 30-50 nm in size. CMEO is rich in total phenolic and flavoniods and showed high antioxidant and radicals scavenging activity *in vitro*. AgNPs disturbed kidney function, decreased the antioxidant enzymes, increased serum electrolytes, TNF-α, MDA and NO, up-regulated Bcl-2, down-regulated Bax and P53 and induced histological changes in kidney tissue. CMEO protected the kidney against AgNPs toxicity in a dose-dependent manner. It could be concluded that AgNPs induced cytotoxicity and oxidative stress in the kidney. CMEO overcomes the nephrotoxicity and should be considered as a supplement to protect the kidney against oxidative stress.

Keywords: *Chenopodium murale*, Silver nanoparticles, Nephrotoxicity, Essential oil, Oxidative stress, Genotoxicity

Introduction

Chenopodium mural is the fastest-growing annuals of Chenopodiaceae family and are widespread throughout various habitat types in Egypt [1]. This plant was introduced to Egypt from the European countries, grows well in the moist soil in winter to early summer and is known as a pest in the agroecosystems and roadsides. It is sometimes eaten as a vegetable and used for food. It is rich in saponin, cyanogenic glycosides, naphthaquinones and tanin, alkaloids, flavonoids and glucose [2]. Several reports showed that the essential oil of *C. mural* is rich in p-cymene and a-terpinene [3-5].

Silver nanoparticles (AgNPs) are used widely in several scientific fields, hygiene, pharmaceutical and biomedical applications because of their unique physicochemical properties [6]. They are excessively used in food packaging [7], seed preservation, biofertilizers and cosmetics [8,9]. They also showed a potent antibacterial [10,11], antimicrobial and anti-proliferative [12,13], antifungal [14], antiviral[15], antioxidant [16] and anticancer properties [17], modulate cytokine and promote wound healing [18].

AgNPs are synthesized using various techniques including chemical or physical

*Corresponding authors e-mail: mosaad_abdelwahhab@yahoo.com; Tel.: +2 2283 1943; fax: +2 3337 0931
ORCID: 0000-0002-7174-3341
Received 17/10/2019; Accepted 17/12/2019
DOI: 10.21608/ejchem.2019.18341.2128

techniques using huge amounts of chemicals under high temperature, consequently the search for alternative safe method is a major request. The synthesis of AgNPs can be done using plant extracts such as *Azadirachta indica*, *Capsicum annuum*, *Gliricidia sepium*, *Carica papaya*, *Eucalyptus hybrida*, *Camellia sinensis* [19-24] and microorganisms including *Aspergillus fumigatus*, *Cladosporium cladosporioides*, *Pseudomonas aeruginosa*, *Fusarium oxysporum* and *Rhodopseudomonas capsulate* [25-29].

The applications of AgNPs may increase the deleterious effects on environment and health of human. The primary or secondary adverse effects of AgNPs on different organs may induce immunotoxicity and neurotoxicity when extend into the CNS (central nervous system) or cardiovascular system [30,31]. AgNPs may accumulate in several human organs, including the liver, spleen, lung, brain, kidney, testicles and heart [32-36]. The accumulation of these nanoparticles in different organs is contributing to severe toxicity since they may induce a status of oxidative stress and the damage to DNA, fatty acids, proteins and cause apoptosis and necrosis [16, 37,38]. Despite their extensive use, the exact toxicity of AgNPs and their adverse effects on the kidney are not well elucidated yet. Therefore, this study aimed to: (1) determination of total phenolic (TP), total falvonoids content (TFC) and antioxidant capacity of *Chenopodium murale* essential oil (CMEO), (2) synthesize and characterize AgNPs using *Chenopodium murale* extract (CME) and (3) assess the genotoxicity and the oxidative stress of AgNPs on kidney and the possible protective activity of CMEO.

Materials and Methods

Chemicals and Kits

Kits for urea was supplied by Prodia Co. (Korbach, Germany). Kits for uric acid, albumin, total protein, catalase (CAT), Na^+, K^+, Mg^{++}, total antioxidant capacity (TAC) and nitric oxide (NO) were supplied by Biodiagnostic Co. (Giza, Egypt), tumor necrosis factor alpha (TNF-α) was supplied by Orgenium (Helsinki, Finland) and malondialdehyde (MDA) was supplied by Oxis Research™ Co. (USA). TRIZOL was obtained from Invitrogen™ (CA, USA), DNA-free ™DNase was obtained from Invitrogen (Germany) and PreMix Kit was obtained from iNtRON Biotechnology (Korea). All other chemicals used throughout the experiments were of analytical grade.

Preparation of Chenopodium murale extract (CME)

The leaves of *Chenopodium murale* (Family: Chenopodiaceae) were collected the agricultural region in Qalubia Governorate, Egypt. The plant was washed and 20 g leaves were boiled in distilled water (50 ml) for 30 min in Erlenmeyer flask, then filtered through filter paper (Whatman # 1) and the filtrate was freeze-dried.

Biosynthesis of AgNPs

CME was used for the synthesis of AgNPs according to Abdel-Aziz et al. [39]. A solution of silver nitrate (3mM) was incubated with CME (50 ml) for 24 h and the change in color to brownish yellow indicated the synthesis of AgNPs as mentioned by Parashar et al. [40].

Characterization of the synthesized AgNPs
UV-vis adsorbance spectroscopy and TEM assay

The formation of AgNPs from $AgNO_3$ was monitored by Shimazu 2401PC UV-vis spectroscopy as described previously [21]. The UV-vis spectrometric reading was recorded at 200-800 nm as described by Leela and Vivekanandan [41]. The TEM analysis was carried out using JEOL model 1200 EX electron microscope and size and shape was determined using TEM micrograph according to Elavazhagan and Arunachalam [42].

Extraction and GC-MS analysis of Chenopodium murale essential oil (CMEO)

Chenopodium murale leaves were mixed with water (1:5 w/v) for hydrodistillation. The distillate was extracted twice with dichloromethane (1:1 v/v). The organic phase was collected and dried with anhydrous sodium sulfate and dichloromethane was evaporated in a rotatory evaporator at 40°C under reduced pressure. The GC-MS analysis of CMEO was carried out using a coupled Varian gas chromatography/ mass spectrometery as described in our previous work [39]. The chemical composition of CMEO showed that hydrodistillation of the plant leaves yielded 0.02% essential oils on a fresh weight basis. The GC-MS and GC analysis using RI resulted in the identification of total of 21 components represented 93.6% of the crude essential oil. The major compounds represented α-Terpinene, (Z)-Ascaridole, trans-Ascaridole, p-Cymene, β-Myrcene, (E)-2-Hexenal, cis-Ascardole and (E)-Ascaridole (40.01%, 32.21%, 4.2%, 2.11%, 1.72%, 1.72%, 2.01% and1.83%, respectively) constituting about 85.82% of the essential oil.

Determination of TFC and TPC of CMEO

TFC and TPC were determined as described by Kim et al. [43] and Singh et al. [44], respectively and the results of TFC were expressed as mg/ g catechin equivalents, whereas; TPC was expressed as mg/g Gallic acid equivalents.

DPPH scavenging activity

The radical scavenging activity of 2, 2-diphenyl-2- picrylhydrazyl (DPPH) was determined as described previously [45]. The absorbance was recorded at 517 nm against a blank and the scavenging activity was calculated as follow:

Inhibition percentage = 100 × (*A* blank - *A* sample/*A* blank)

Where:

A blank: absorbance of control reaction which contain all reagents without the test compound)

A sample: absorbance of the tested compound.

β-Carotene bleaching assay

β-carotene was determined as previously described [46] and the calculation was done as follow:

Antioxidant activity = $1-(A_0-A_t)/ (A^0_0-A^t_0)$

Where:

A_0 and A^0_0: absorbance values at initial time of samples and control, respectively.

A_t and A^t_0: absorbance of the samples and the control at t = 120 min, respectively.

Experimental animals

Sexually mature female Sprague-Dawley rats (3 months old, 150-160 g) were obtained from the Animal House colony, National Research (NRC) Center, Dokki, Cairo, Egypt. The animals were fed a standard pellet diet and housed in polycarbonate cages in a room artificially illuminated and thermally controlled ((12 h dark/ light cycle, 25 ± 1 ^{O}C) and free from any source of chemical contamination at the Animal House Lab, NRC, Dokki, Cairo, Egypt. All animals were received the humane care in compliance with the guidelines of the National Institute of Health (NIH publication 86-23 revised 1985) and the protocol was approved by the Animal Care and Use Committee of NRC, Dokki, Cairo, Egypt.

Experimental design

A total of 70 female rats were distributed into 7 groups and treated orally for 3 weeks as follows: group1; control group, groups 2 and 3; rats received low dose (LD) and high dose (HD) of o.5 ml aqueous solution of AgNPs (25 and 50 mg/kg b.w), groups 4 and 5; rats treated with low dose (LD) or high dose (HD) of CMEO (0.5 and 1 mg/kg b.w) and groups 6 and 7; rats treated with AgNPs plus CMEO (LD) or CMEO (HD). After the termination of the experimental period (i.e. day 21), samples of blood were collected under diethyl ether anesthesia through the retro-orbital venous plexus from all animals after being fasting for 12 hr. The blood samples were centrifuged at 1700 rpm and 4^{O}C and sera were collected and stored at -20 ^{O}C. The serum samples were used for the determination of creatinine, urea, uric acid, total protein, albumin, NO and TNF-α as shown in the manufacturer's instructions. Serum electrolytes concentrations including sodium (Na^+) and potassium (K^+) were determined as described by Henry [47]. However, serum magnesium (Mg^{+2}) was measured colorimetrically [48].

All rats within different experimental groups were sacrificed after the collection of blood samples and kidney samples were collected. Three samples of kidney were gathered from each rat. The first sample was weighted and homogenized in phosphate buffer according to Lin et al. [49]. The homogenate (20 % w/v) was cooling centrifuged for 10 min at 1700 rpm and the supernatant was used for MDA assay based on the manufacture instaurations. Then the supernatant was further diluted using phosphate buffer to 2% and 0.5% for CAT and TAC assay, respectively based on the manufacturer's instructions. The second kidney sample from each rat was fixed in 10% natural formalin for the histological examination as described by Drury and Wallington [50]. However, the third kidney sample was used for the cytogenetic studies.

Cytogenetic analysis

Acridine orange/ethidium bromide for apoptosis assay

The renal cells apoptotic was determined by morphologic examination using fluorescent microscopy as described by Thakur and Sanyal [51]. One hundred cells were examined and were classified as early apoptotic cells, late apoptotic cells and necrotic cells based on the broken chromatin and the nucleus color. The necrotic/ apoptotic ratio was calculated by dividing the number of apoptotic or necrotic cells by the total cell counts x 100.

Extraction of Total RNA

Total RNA was extracted from the frozen kidney tissue using TRIZOL reagent as described previously [52]. The purity of the total RNA was estimated by the ratio of 260/280 nm (between 1.8 and 2.1) and the integrity was analyzed by ethidium bromide-stain of 28S and 18S bands. The RNA aliquots were used for reverse transcription (RT).

RT and sq-PCR

The sq-PCR was performed by the reverse-transcribed of 1 µg of the isolated total RNA into cDNA with the RT PreMix Kit as indicated by the manufacturer's instructions. A sqRT-PCR was used for the estimation of tested gene expressions (Bax, Bcl2 and P53). The determination of rat cDNA copy number was assessed as described previously [52]. The PCR mixture consisted of cDNA 2 µl, 10× PCR buffer 2 µl, dNTPs 2 µl, Taq DNA polymerase 0.2 µl, forward/reverse primer 0.2µl and 0.1% diethylpyrocarbonate water for final volume 20 µl were amplified as follows: denaturation at 94 ^{o}C for 3 min and 94 ^{o}C for 30s, annealing from 56-58 ^{o}C for 30s, extension at 72 ^{o}C for 30s (30 cycles) and final extension at 72 ^{o}C for 5 min. The primer sequences used in this study and cycling conditions are summarized in Table (1).

sq-PCR

The PCR product was run on a 1.5% agarose gel in Tris-borate-EDTA buffer then visualized over a UV Trans-illuminator. The bands were quantified by computerized Gel-Pro software (version 3.1 for window 3) and the ratio between GAPDH as an internal control and the levels of amplification product of the target gene was calculated as described by Raben et al. [53]. All PCRs were done in independent triplicates.

Statistical analysis

The data were subjected to analysis of Variance (ANOVA) using GLMP (the General Linear Model Procedure) of SAS [54]. The significances between different treatment groups were determined according to Waller and Duncan [55]. The statements of the significance were based on probability of $P \leq 0.05$.

Results

The current results revealed that the incubation of 50 ml of 3 mM $AgNO_3$ with 5 ml of CME for 24 h at the room temperature led to the synthesis of AgNPs as indicated by the development of the brown color (Fig. 1a). The maximum absorption of the developed brown color by the spectrophotometric analysis ranged from 450-500 nm (Fig. 1b). Moreover, the TEM scan showed that AgNPs the average particles sizes was 40 ± 0.4 nm and ranged from 30 to 50 nm (Fig. 1c).

The results showed that TPC and TF in CMEO were 75.2 mg/g GAE and 13.21 mg/g catechin, respectively. Additionally, the antioxidant properties of CMEO as determined using β-carotene bleaching assays and DPPH scavenging revealed that both DPPH values and β-carotene oxidation were increased significantly by the increase of CMEO doses (Table 2).

The *in vivo* results indicated that serum creatinine, uric acid and urea were significantly increased in animals treated with AgNPs at the low or high dose while the levels of albumin and

TABLE 1. Oligonucleotide primers used for analysis of apoptotic genes by reverse-transcriptase polymerase chain reaction (PCR)

Primer	Primer sequences	Conditions	Ref.
Bax	F: 5′-AGGATGATTGCTGATGTGGATAC-3′ R: 5′-CACAAAGATGGTCACTGTCTGC-3′	94 ^{o}C 3 min (94, 30 sec; 56, 30 sec; 72, 30 sec) ×30	Van Der Hoeven et al. (2003)
Bcl-2	F: 5′-GCTACGAGTGGGATACTGGAGA-3′ R: 5′-AGTCATCCACAGAGCGATGTT-3′	94 ^{o}C 3 min (94, 30 sec; 58, 30 sec; 72, 30 sec) ×30	Van Der Hoeven et al. (2003)
P53	F: 5′-GCACAAACACGCACCTCAAAGC -3′ R: 5′-CTTGCATTCTGGGACAGCCAAG-3	94 ^{o}C 3 min (94, 30 sec; 57, 30 sec; 72, 30 sec) ×30	Kurtulus et al. (2012)
GAPDH	F: 5′- AAGGTCATCCATGACAACTTTG -3′ R: 5′-TCCACCACCCTGTTGCTGTAG -3′	94 o C 3 min (94, 30 sec; 58, 30 sec; 72, 30 sec) ×35	Wiame et al. (2000)

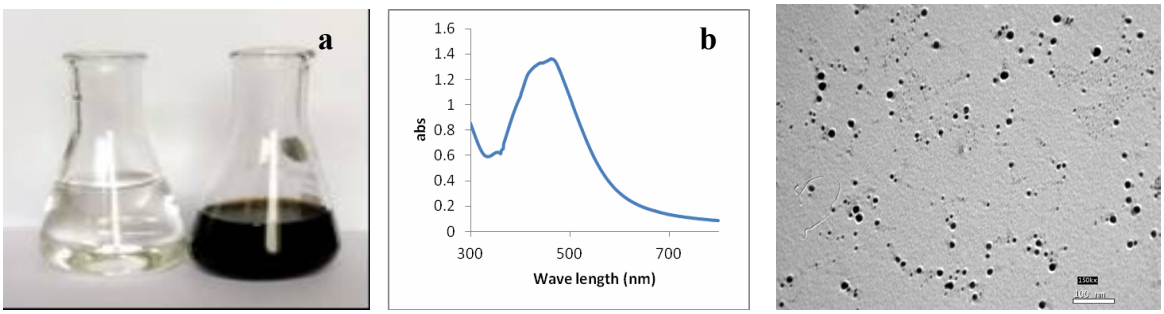

Fig. 1. (a) Changes of AgNO3 color to reddish-brown after the addition of *C. murale* leaves extract; (b) The Uv/Vis absorbance at 460 nm for the produced solution and (c) The transimittance electron microscope (TEM) image of AgNPs showing that the particles were in the nano form with average sizes of 30-50 nm.

TABLE 2. Total phenolic, total flavoniods, DPPH radical scavenging activity and β-carotene CMEO

TPC (mg/g GAE eq)	TF (mg/g catechin eq)	DPPH radical scavenging activity (%)	β-carotene (%)
75.2 ± 0.12	13.21 ± 0.16	62.33 ± 0.74	52.74 ± 0.55

TPC: total phonic content; TF: total flavoniods

total protein were significantly decreased. These changes were more pronounced in the group received AgNPs (HD) compared to those of the control group (Table 3). Animals received CMEO alone were comparable to the control except uric acid which was decreased significantly in a dose dependent manner. Moreover, the co-administration of CMEO plus AgNPs decreased significantly the level of uric acid compared to AgNPs alone-treated groups and succeeded to normalize the levels of creatinine, total protein and albumin.

The results presented in Table (3) also indicated that administration of AgNPs (LD) or AgNPs (HD) increased serum NO in a dose dependent manner, however; animals treated with CMEO (LD) or CMEO (HD) did not induce any significant changes in NO level compared to the normal control animals. Co-treatment with the low or high dose of AgNPs plus CMEO improved significantly NO level towards the control values, however; these values were still higher than the control. Additionally, AgNPs alone increased TNF-α in a dose dependent manner. Treatment with CMEO (LD) or CMEO (HD) alone induced a significant decrease in TNF-α and the combined treatment with AgNPs plus CMEO (LD) or AgNPs plus CMEO (HD) improved TNF-α significantly compared to AgNPs alone and the group treated with AgNPs plus CMEO (HD) was significantly lower than the control group (Table 3).

The data presented in Table (4) revealed that treatment with AgNPs (LD) or AgNPs (HD) significantly increased renal MDA and decreased CAT and TAC in a dose dependent manner. Treatment with CMEO (LD) or CMEO (HD) alone induced a significant decrease in renal MDA but did not affect CAT and TAC significantly. Moreover, co-administration of AgNPs plus CMEO (LD) or AgNPs plus CMEO (HD) could improve the level of MDA and normalized the antioxidant parameters (Table 4). It is also clear that the improvement in MDA, TAC and CAT was dose dependent.

Serum electrolytes (Table 5) showed a significant increase in Na^+, K^+, Mg^{++} in the groups received AgNPs(LD) or AgNPs(HD), whereas; treatment with CMEO (LD) or CMEO (HD) decreased significantly serum Na^+ but K^+ and Mg^{++} were within the normal control level. Co-treatment with CMEO plus AgNPs improved significantly all serum electrolytes and treatment with AgNPs plus CMEO (HD) could normalize K^+ level.

The fluorescence microscopic analysis of renal cells showed alterations in the morphological shape and an increase in necrosis/ apoptotic ratio in rats treated with AgNPs (LD) or AgNPs (HD) compared with control (Fig. 2 A-D). However, treatment with CMEO (LD) or CMEO (HD)

TABLE 3. Effect of CMEO on serum biochemical endpoints in rats treated with AgNPs

Parameter / Groups	Creatinine (mg/dl)	Uric acid (mg/dl)	Urea (mg/dl)	T. P (g/L)	Albumin (g/L)	TNFα (mg/L)	NO (µmol/L)
Control	0.92 ± 0.15[a]	1.75 ± 0.08[a]	34.87± 2.37[a]	5.88 ± 0.48[a]	3.46 ± 0.22[a]	94.41 ± 0.84[a]	7.02 ± 0.49[a]
AgNPs (LD)	1.37 ± 0.06[b]	2.13 ± 0.19[b]	37.14 ± 2.22[b]	3.58 ± 0.31[b]	2.45 ± 0.11[b]	117.57 ± 3.92[b]	11.96 ± 0.45[b]
AgNPs (HD)	1.97 ± 0.08[c]	3.95 ± 0.36[c]	39.40 ± 3.67[c]	2.08 ± 0.87[c]	1.50 ± 0.32[c]	127.85 ± 9.99[c]	16.96 ± 0.22[c]
CMEO (LD)	1.06 ± 0.07[a]	1.29 ± 0.18[d]	33.85 ± 4.31[a]	5.68 ± 0.69[a]	3.87 ± 0.26[a]	82.28 ± 3.9[d]	6.88 ± 0.55[a]
CMEO (HD)	1.02 ± 0.05[a]	1.50 ± 0.22[e]	33.71 ± 4.43[a]	5.08 ± 0.17[a]	3.59 ± 0.10[a]	88.28 ± 3.19[e]	6.78 ± 0.41[a]
AgNPs + CMEO (LD)	0.97 ± 0.05[a]	1.65 ± 0.13[a]	33.08 ± 2.61[a]	5.88 ± 0.25[a]	3.50 ± 0.12[a]	102.28 ± 7.16[f]	7.75 ± 0.21[a]
AgNPs + CMEO (HD)	0.89 ± 0.06[a]	1.71 ± 0.19[a]	30.91 ± 3.82[d]	6.15 ± 0.20[a]	3.60 ± 0.12[a]	90.28 ± 0.99[e]	7.63 ± 0.70[a]

Within each column, means superscript with different letters (a, b, c…..) are significantly different (P≤0.05)
Results are mean ± SE

TABLE 4. Effect of CMEO on MDA, catalase and total antioxidant capacity in kidney of rats treated with AgNPs

Parameter / Groups	MDA (mol/mg protein)	CAT (U/mg protein)	TAC (mM/mg protein)
Control	17.94 ± 0.60[a]	585.87 ± 26.39[a]	2.39 ± 0.19[a]
AgNPs (LD)	27.80 ± 1.56[b]	460.44 ± 53.56[b]	1.43 ± 0.13[b]
AgNPs (HD)	39.50 ± 1.48[c]	420.74 ± 30.64[c]	0.84 ± 0.13[c]
CME (LD)	15.99 ± 2.63[d]	580.79 ± 66.28[a]	2.41 ± 0.15[a]
CME (HD)	15.30 ± 0.97[d]	582.94 ± 35.38[a]	2.46 ± 0.25[a]
AgNPs + CME (LD)	20.32 ± 1.47[e]	665.14 ± 30.22[d]	2.42 ± 0.18[a]
AgNPs + CME (HD)	22.41 ± 1.77[f]	649.02 ± 30.11[e]	2.41 ± 0.19[a]

Within each column, means superscript with different letters (a, b, c…..) are significantly different (P≤0.05)
Results are mean ± SE

TABLE 5. Effect of CMEO on serum electrolytes in rats treated with AgNPs

Parameter / Groups	Na^+ (mM/L)	K^+ (mM/L)	Mg^{++} (mM/L)
Control	124.0 ± 3.14[a]	3.98 ± 0.27[a]	1.37 ± 0.10[a]
AgNPs (LD)	142.86 ± 2.12[b]	5.07 ± 0.19[b]	3.17 ± 0.07[b]
AgNPs (HD)	160.14 ± 5.79[c]	8.66 ± 0.38[c]	4.68 ± 0.05[c]
CMEO (LD)	117.29 ± 4.74[d]	3.83 ± 0.39[a]	1.46 ± 0.09[a]
CMEO (HD)	111.29 ± 5.75[e]	3.94 ± 0.42[a]	1.44 ± 0.13[a]
AgNPs + CMEO (LD)	108.57 ± 4.55[d]	3.94 ± 0.13[a]	1.36 ± 0.07[a]
AgNPs + CMEO (HD)	149.57 ± 3.07[f]	3.97 ± 0.35[a]	1.81 ± 0.10[d]

Within each column, means superscript with different letters (a, b, c…..) are significantly different (P≤0.05)
Results are mean ± SE

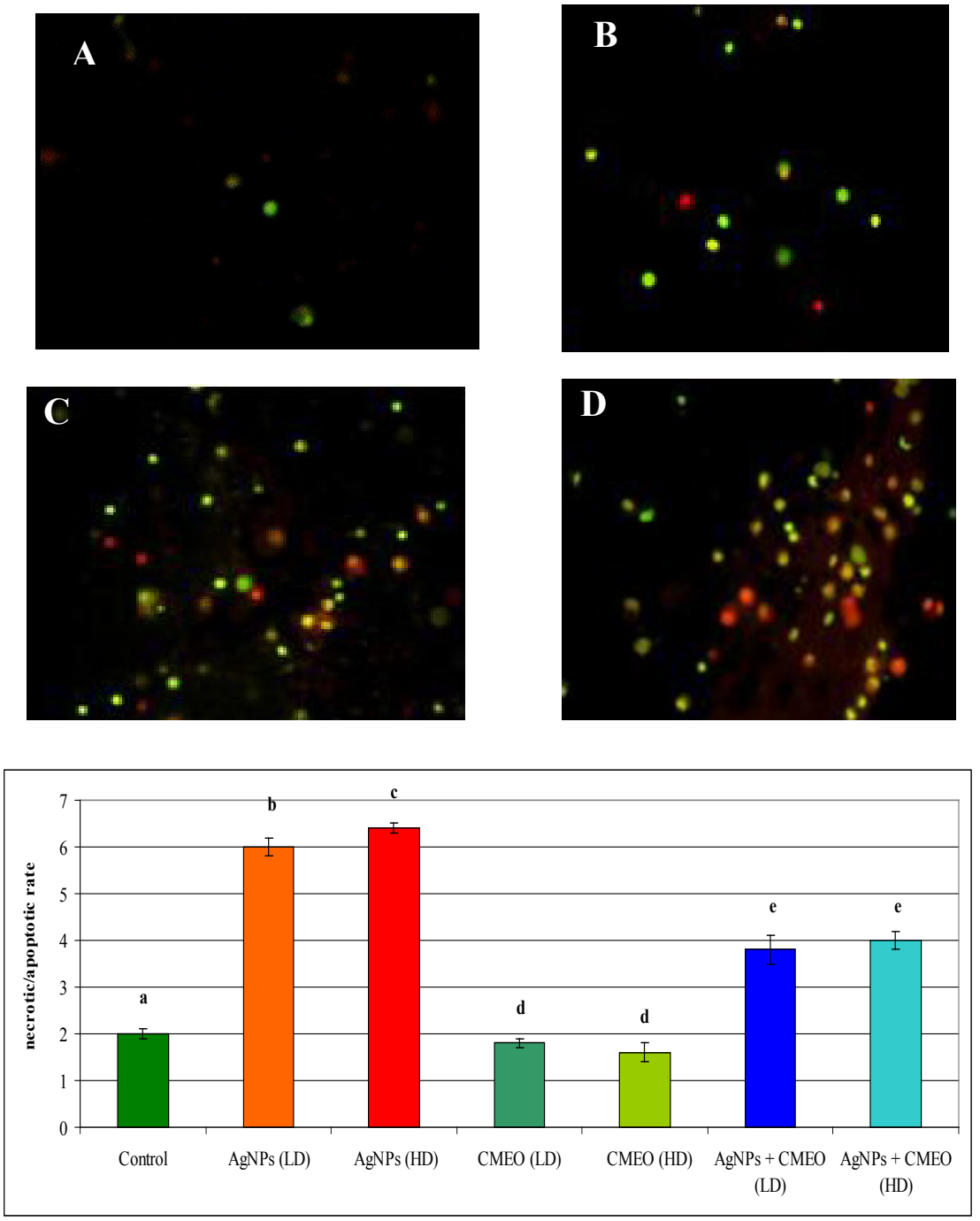

Fig. 2. Renal cells under fluorescence microscope (20X). as assessed by Ethidium Bromide/Acridine Orange co-staining- viable cells stain uniformly green, (A) Negative control group (normal cells, CMEO): the circular nucleus uniformly distributed in the center of the cell. (B) Experimental group (early apoptotic cells) (AgNPs (LD)): nucleus showed yellow-green fluorescence by acridine orange (AO) staining and concentrated into a crescent or granular that located in 1 side of cells. (C, D) Experimental group (late apoptotic cells) AgNPs (HD): the nucleus of cell showed orange fluorescence by EB staining and gathered in concentration and located in bias. The necrosis cells' volume was increased, showing uneven orange-red fluorescence and an unapparent outline. It is becoming dissolved or near disintegration. (E) Effect of CMEO in induction of necrotic/apoptotic rate in renal cells of AgNPs-treated rats

Within each column, means superscript with different letters (a, b, c…..) are significantly different (P≤0.05)

decreased significantly the necrosis/apoptotic ratio than the control or the AgNPs-alone treated rats. Administration of AgNPs plus CMEO (LD) or AgNPs plus CMEO (HD) significantly decreased the elevation of necrosis/apoptotic ratio but no significant change was noticed between the animals received CMEO (LD) or HD alone and those received AgNPs plus CMEO at the two tested doses (Fig. 2 E).

The effect of different treatments on mRNA expression of the anti-apoptotic gene (Bcl-2) and the pro-apoptotic gene (Bax) showed that administration of AgNPs at both low and high dose down-regulated renal Bcl-2 mRNA (Fig. 3a) and up-regulated Bax mRNA expression (Fig. 3b) in a dose dependent fashion. However; no significant effect was observed in P53 mRNA expression (Fig. 3c) in the animals received CMEO alone at either low or high doses. Co-administration of CMEO plus AgNPs at the low or high doses improved significantly the expression of all investigated genes. These treatments did not normalize the expression of the tested genes since they are still significantly differing than the control animals.

The microscopic examination of the sections of control kidney cortex showed normal renal corpuscle, parietal layers of Bowman's capsule, glomerulus and preserved renal space as well as normal proximal and distal convoluted tubules (Fig. 4a). The renal sections of rats received AgNPs (LD) showed an increase in the number of abnormal glomeruli (shrunken or atretic or necrotic) and focal of necrotic tubules (Fig. 4b.). Examination of renal cortex of the groups received AgNPs (HD) showed an increase in the interstitium spaces, infiltration and hemorrhage with focal tubular sclerosis (Fig. 4c). The renal cortex of rats received CMEO (LD) showed few foci of infiltration and/or tubular necrosis with pyknotic nuclei (Fig. 4d). However the renal cortex of rats received CMEO (HD) showed foci of tubular epithelial cell necrosis with pyknotic nuclei, most of the tubules showed eosinophilic cytoplasm and intact epithelial cells

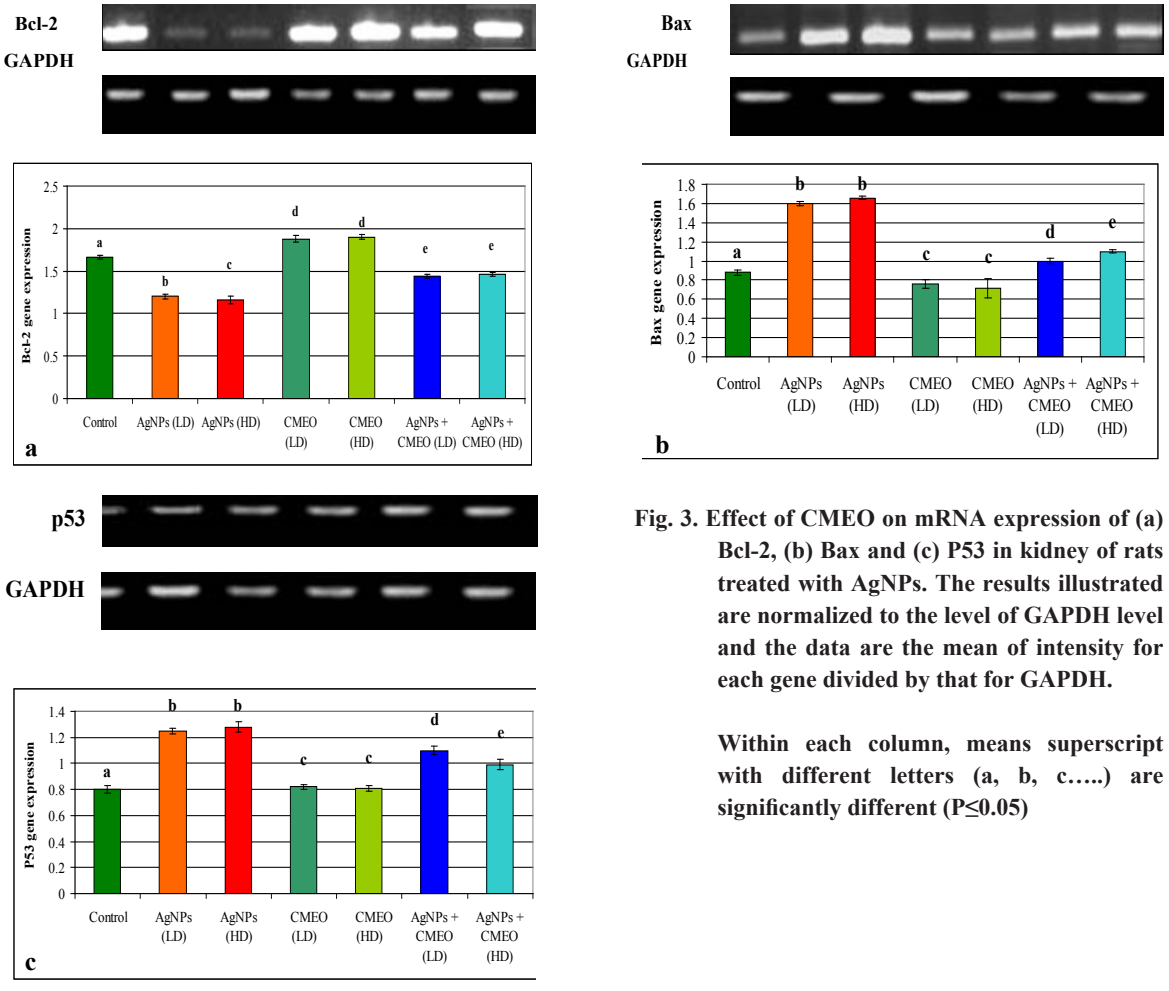

Fig. 3. Effect of CMEO on mRNA expression of (a) Bcl-2, (b) Bax and (c) P53 in kidney of rats treated with AgNPs. The results illustrated are normalized to the level of GAPDH level and the data are the mean of intensity for each gene divided by that for GAPDH.

Within each column, means superscript with different letters (a, b, c…..) are significantly different (P≤0.05)

(Fig. 4e). The kidney sections of the rats received AgNPs plus CMEO (LD) showed pronounced regeneration in renal tubules and glomeruli, most of the tubules showed eosinophilic cytoplasm, intact epithelial cells, Glomeruli with the parietal layer of Bowman's capsule and preserved renal spaces (Fig. 4f). The sections of cortex of the rat kidney received AgNPs plus CMEO (HD) showed pronounced regeneration in renal tubules and glomeruli, most of tubules showed eosinophilic cytoplasm and intact epithelial cells. Additionally, the atretic Glomeruli were decreased, but still segmented with dark stained mesangial cell nuclei (Fig. 4g).

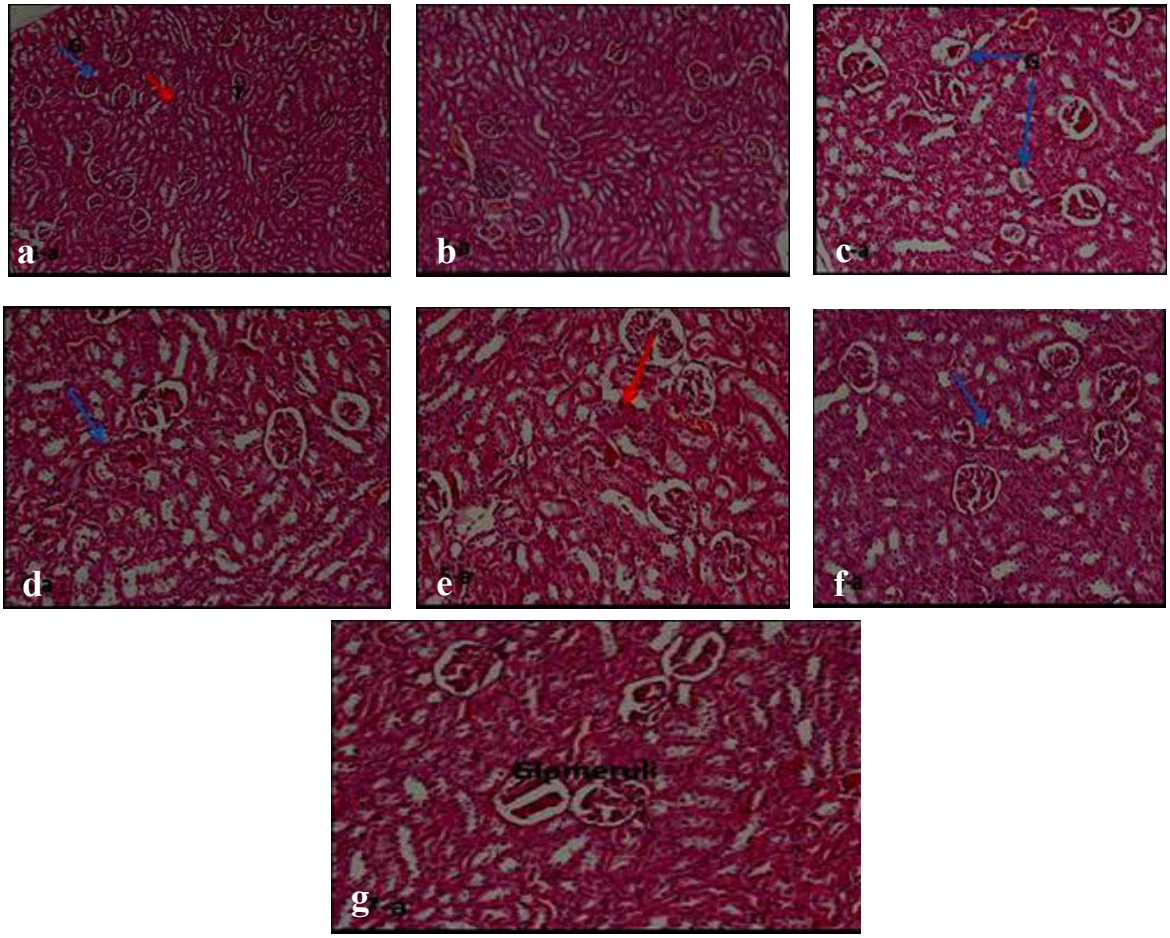

Fig. 4. A photomicrograph of the kidney cortex sections of (a) control rat showing the renal corpuscle with parietal layer of Bowman's capsule, glomerulus (G), preserved renal space and proximal and distal convoluted tubules (T); (b) rats treated with AgNPs (LD) showing increase in the number of abnormal glomeruli (shrunken or atretic or necrotic) and focal of necrotic tubules, (c) rats treated with AgNPs (HD) showing increase in the interstitium spaces of infiltration and hemorrhage with focal tubular sclerosis; notice that the glomeruli less affected, (d) rats treated with CMEO (LD) showing foci of infiltration and/or tubular necrosis with pyknotic nuclei; notice that the few glomeruli are affected, (e) rats treated with CMEO (HD) showing foci of tubular epithelial cell necrosis with pyknotic nuclei, most of tubules appeared with eosinophilic cytoplasm and intact epithelial cells; notice that the glomeruli with the parietal layer of Bowman's capsule and preserved renal spaces, (f) rats treated with AgNPs + CMEO (LD) showing pronounced regeneration in renal tubules and glomeruli, most of tubules appeared with eosinophilic cytoplasm and intact epithelial cells; the glomeruli with the parietal layer of Bowman's capsule and preserved renal spaces; notice the epithelial apoptotic nuclei (arrow) and (g) rats treated with AgNPs + CMEO (HD) showing pronounced regeneration in renal tubules and glomeruli, most of tubules appeared with eosinophilic cytoplasm and intact epithelial cells; the atretic glomeruli are decreased but still segmented with dark stained mesangial cell nuclei. (HX & E. X 200)

Discussion

We applied the green chemistry to synthesize AgNPs using *Chenopodium murale* leaves extract (CME). The change in the color of $AgNO_3$ after the incubation with CME for 24 h in the dark indicated the ability of CME to reduce $AgNO_3$ to AgNPs. This result has been observed previously and indicated that the change in color maybe appeared due to the surface plasmon resonance of the deposited AgNPs [39,56]. The TEM results confirmed the formation of AgNPs and showed that the synthesized nanoparticles have a size ranged from 30-50 nm.

The present results revealed that CMEO is rich in TPC and TF. Previous reports indicated that phenolic compounds are directly contributed to the antioxidant activities [57]. These antioxidant properties of the plant phenolic compounds are primarily due to redox properties of these compounds, which enable them to donate hydrogen, act as singlet oxygen quenchers and reducing agents as mentioned previously [58]. To the best of our knowledge, no available published data about the TPC in *Chenopodium murale*, however; Laghari et al. [59] reported that *Chenopodium album* is rich in TPC and the plants in *Chenopodiaceae* family are rich in TPC and TFC with a potential antioxidant activity [60].

The results of DPPH scavenging and β-carotene bleaching assays indicated the increased in DPPH values by increasing the dose of the extract. Similarly, Nsimba et al. [61] showed that other spices of *Chenopodiaceae* family i.e. *Chenopodium quinoa* and *Chenopodium album* have a high antioxidant activity.

In the biological experiment, the nephrotoxicity of synthesized AgNPs and the preventive role of CMEO were evaluated in rats. AgNPs administration induced severe disturbances in kidney function indices, increased NO and MDA, decreased the activity of the antioxidant enzyme in the renal tissues and disturb the expression of Bax, Bcl-2 and P53 mRNA and induced severe histological changes in the kidney cortex. Although the toxic effects of nanomaterials mainly depend on the characteristics of the particles, the current study indicated that the particle size of 30-50 nm is critical and induce toxic effects to the kidney. These findings are in agreement with the previous reports which suggested that the liver and kidney are the target organs for AgNPs toxicity and ingestion of AgNPs induced a significant elevation in the liver and the kidney function indices [62]. Moreover, the reduction in albumin and total protein levels suggested the impairment of kidney function [63].

The significant decrease in renal CAT and TAC along with the elevation in renal MDA, serum NO and TNF-α together with the disturbances in mRNA of Bax, Bcl-2 and P53 expression in rats ingested AgNPs suggested the induction of oxidative stress and supported the previous reports [16,64-66]. It was reported that ROS generation is the important mechanism for the toxicity of AgNPs [67]. Oxidative stress is considered the subsequent generation of the inflammatory mediators, apoptosis and DNA damage [68,69]. Kim et al. [70] reported that the increase in ROS and MDA levels, and the decrease GPx after AgNPs administration are considered the mechanisms of organ damage. Additionally, Song et al. [71] reported that AgNPs cause damage of the membrane, LDH leakage, reduce the activity of GPx and SOD and the cell viability in the human hepatoma cell line HL-7702. Three major mechanisms were suggested for the toxicity of AgNPs included: generation of oxidative stress [72], the damage to DNA [73] and the induction of cytokine [74]. Based on these mechanisms, AgNPs can internalize by the scavenger receptors and trafficked to the cytoplasm and consequently the release of Ag ions and the induction the toxicity. Thus the presence of reactive silver ion and thiol-containing compounds are the predisposing conditions for the toxicity of AgNPs [75]. The alterations in the morphological shape and the increase in necrosis/ apoptotic ratio along with the histological changes reported herein in rats received AgNPs at the two tested doses indicated the severe cytotoxicity in the kidney even at the low dose. These findings were in accordance with the previous studies [76-80].

In addition, the present results also showed that sodium (Na^+) and magnesium (Mg^{++}) levels were increased significantly and potassium (K^+) level was significantly declined. Similar to these results, Heydrnejad and Samani [81] suggested that AgNPs affect the sodium/potassium pump which maintains the constant concentration of Na^+ or K^+ electrolytes in extracellular fluids and reflect the early kidney stress [82-84].

The results also indicated that administration of CMEO alone did not induce any significant effects on serum and tissue biochemistry, the cytogenetic and the tissue histology. Meanwhile,

it elevated the antioxidants, modulates the gene expression, decreased the cytokine and suppressed generation of ROS; consequently, prevents the subsequent kidney damage [85]. Similarly, Lin et al. [86] suggested that the plants in *Chenopodiaceae* family protect against the oxidative damage due to the high content of polyphenols, saponins and alkaloids which have free radical scavenging properties and antioxidant activities. Furthermore, Chang et al. [58] concluded that the antioxidant of the phenolic compounds is primarily attributed to their redox properties, ability to donate hydrogen, reducing agents and singlet oxygen quenchers. CMEO also up-regulated Bcl-2 expressions, down-regulates Bax and P53 expression and decreased TNF-α suggesting the anti-inflammatory properties of this plant through the elimination of ROS generation which is responsible for the inflammation process [85]. Moreover, Gawlik-Dziki et al. [87] reported that CMEO is rich in quercetin and other phenolics which are well documented as antioxidants including free radical scavenging, metal chelation, reducing power, protect against lipid peroxidation and lipoxygenase activity. The current findings are consistent with the previous reports which have reported that the antioxidant effects of essential oils are mainly due to TFC and TPC [39, 88], tannin and steroid [89,90]. Taken together, the reinforcement of the antioxidant system along with the free radical scavenging properties leads to positive curative effects against kidney injury [91].

Conclusion

The current study concluded that CMEO is rich in TF and TPC and has a potential antioxidant and radical scavenging activity. AgNPs with particles size of 30-50 nm can be synthesized using CME. The synthesized AgNPs induced renal toxicity as manifested by the negative effects on the kidney function indices, serum electrolytes, oxidative stress markers, cytokines and antioxidant parameters. AgNPs also induced morphological changes and an increase in necrosis/ apoptotic in the kidney cells, disturb the expression of Bax, Bcl-2 and P53 expressions indicating a renal cytotoxicity. CMEO is a promising candidate that can help in the chemoprevention against AgNPs and other disorder related to oxidative stress due to the higher content of flavonoids and phenolic compounds responsible for the antioxidant activity.

Acknowledgments

This work was supported by the National Research Center, Dokki, Cairo, Egypt, Project # 12050305.

Declarations of interest

none

References

1. Shaltout KH, Sharaf El-Din A, El-Fahar RA. Weed communities of the common crops in the Nile Delta region. Flora **187**, 329-339 (1992)

2. Verma S, Agarwal P. Phytochemical investigation of *Chenopodium album* Linn. and *C. murale* Linn. National Academy of Sciences, *Sci Lett.* **8(5),** 137-138 (1985).

3. Onocha PA, Ekundayo O, Eramo T, Laakso I. Essential oil constituents of *Chenopodium ambrosioides* L. leaves from Nigeria. *J Essent Oil Res.* **11**, 220-222 (1999).

4. Gupta D, Charles R, Mehta VK, Garg AN, Kumar S. Chemical examination of the essential oil of *Chenopodium ambrosioides* L from the southern hills of India. *J Essent Oil Res.* **14,** 93-94 (2002).

5. Tapondjou LA, Adler C, Boud AH, Fontem DA. Efficacy of powder and essential oil from *Chenopodium ambrosioides* leaves as post-harvest grain protectants against six-stored product beetles. *J Stored Products Res.* **38**, 395-402 (2002).

6. Marin S, Vlasceanu GM, Tiplea RE, Bucur IR, Lemnaru M, Marin MM, Grumezescu AM. Applications and toxicity of silver nanoparticles: a recent review. *Curr Topic Med Chem.* **15(16)**, 1596-604 (2015).

7. Deshmukh SP, Patil SM, Mullani SB, Delekar SD. Silver nanoparticles as an effective disinfectant: A review. *Mater Sci Eng C Mater Biol Appl.* **97,** 954-965 (2019).

8. Dipankar C, Murugan S. The green synthesis, characterization and evaluation of the biological activities of silver nanoparticles synthesized from *Iresine herbstii* leaf aqueous extracts. *Colloids Surf B Biointerface* **98,** 112-11(2012). doi: 10.1016/j.colsurfb.2012.04.006

9. Marambio-Jones C, Hoek EMV. A review of the antibacterial effects of silver nanomaterials and potential implications for human health and the environment. *J Nanoparticle Res.* **12**, 1531-1551 (2010). doi: 10.1007/s 11051-010-9900-

10. Mohanta Y, Panda S, Biswas K, Tamang A, Bandyopadhyay J, Mohanta D, et al. Biogenic synthesis of silver nanoparticles from *Cassia fistula* (Linn.): in *vitro* assessment of their antioxidant, antimicrobial and cytotoxic activities. *IET Nanobiotechnol.* **10**, 438-444 (2016a). doi: 10.1049/iet-nbt.2015.0104.

11. Mohanta Y, Singdevsachan S, Parida U, Panda S, Mohanta T, Bae H. Green synthesis and antimicrobial activity of silver nanoparticles using wild medicinal mushroom *Ganoderma applanatum* (Pers.) pat. from similipal biosphere reserve. Odisha, India. *IET Nanobiotechnol* **10,** 184-189 (2016b). doi: 10.1049/iet

12. Sadeghi B, Garmaroudi FS, Hashemi M, Nezhad HR, Nasrollahi A, Ardalan, S. Comparison of the anti-bacterial activity on the nanosilver shapes: nanoparticles, nanorods and nanoplates. *Adv Powder Technol* **23**(1), 22-26(2012).

13. Nayak D, Ashe S, Rauta PR, Kumari M, Nayak B. Bark extract mediated green synthesis of silver nanoparticles: evaluation of antimicrobial activity and antiproliferative response against osteosarcoma. *Mater Sci Eng C Mater Biol Appl*. ***58***, 44-52 (2016.). doi: 10.1016/j.msec.2015.08.022

14. Kim YS, Kim JS, Cho HS, Rha DS, Kim JM, Park JD, et al. Twenty-eight-day oral toxicity, genotoxicity and gender related tissue distribution of silver nanoparticles in Sprague Dawley rats. *Inhal Toxicol.* **20**(6), 575-583(2008).

15. Mehrbod P, Motamed N, Tabatabaian M, Soleimani R, Amini E, Shahidi M, et al. *In vitro* antiviral effect of nanosilver on influenza virus. *DARU* **17**, 88-93(2009).

16. Abdel-Wahhab MA, Ahmed HM, Abdel-Aziem SH, El-Nekeety AA, Abd El-Kader HMA, Abdel-Aziz MS, et al. Modulation of hepatotoxicity, DNA fragmentation and gene expression of *Solanun nigrum* leaves extract in rats treated with silver nanoparticles. *J Appl Pharm Sci.* **7** (2), 025-035 (2017).

17. Nayak D, Pradhan S, Ashe S, Rauta PR, Nayak B. Biologically synthesised silver nanoparticles from three diverse family of plant extracts and their anticancer activity against epidermoid A431 carcinoma. *J Colloid Interf Sci.* **457**, 329-338 (2015). doi: 10.1016/j.jcis.2015.07.012

18. Wong KK, Cheung SO, Huang L, Niu J, Tao C, Ho CM. Further evidence of the anti-inflammatory effects of silver nanoparticles. *ChemMedChem* **4**, 1129-1135 (2009).

19. Shankar SS, Rai A, Ankamwar B, Singh A, Ahmed A, Sastry M. Biological synthesis of triangular gold nonoprism. *Nat Mater* **3,** 482-488 (2004).

20. Bar DK, Bhui GP, Sahoo P, Sarkar SP, De A, Misra A. Green synthesis of silver nanoparticles using latex of *Jatropha curcas*. *Colloids Surf A: Biointerf* **339**,134-139(2009).

21. Raut RW, Kolekar NS, Lakkakula JR, Mendhulkar VD, Kashid SB. Extracellular synthesis of silver nanoparticles using dried leaves *of Pongamia pinnata* (L) Pierre. *Nano-Micro Lett.* **2**, 106-113(2010).

22. Jha AK, Prasad K. Green synthesis of silver nanoparticles using *Cycas* leaf. *Int J Green Nanotechnol: Physic Chem*. **1**, 110-117(2010).

23. Dubey M, Bhadauria S, Kushwah BS. Green synthesis of nanosilver particles from the extract of *Eucalyptus hybrid* (Safeda leaves). *Dig J Nanomater Biostruct* **5**, 537-543 (2009).

24. Vilchis-Nestor AR, Sánchez-Mendieta V, Camacho-López MA, Gómez-Espinosa RM, Camacho-López MA, et al. Solventless synthesis and optical properties of Au and Ag nanoparticles using *Camellia sinensis* extract. *Mater Lett.* **62**, 3103-3105 (2008).

25. Ahmad A, Mukherjee P, Senapati S, Mandal D, Khan MI, Kumar R, et al. Extracellular biosynthesis of silver nanoparticles using the fungus *Fusarium Oxysporum*. *Colloids surf Biointerfaces* **28**, 313-318(2003).

26. Balaji DS, Basavaraja S, Deshpande R, Bedre Mahesh D, Prabhakar BK, Venkataraman A. Extracellular biosynthesis of functionalized silver nanoparticles by strains of *Cladosporium Cladosporioides* fungus. *Colloids Surf B: Biointerfaces* **68**(1), 88-92(2009).

27. Bhainsa KC, D'Souza SF. Extracellular biosynthesis of silver nanoparticles using the fungus *Aspergillus fumigatus*. *Colloids Surf B: Biointerfaces* **47**,160-164 (2006).

28. He S, Guo Z, Zhang Y, Zhang S, Wang J, Gu N. Biosynthesis of gold nanoparticles using the bacteria *Rhodopseudomonas capsulata*. *Mater Lett* **61** (18), 3984-3987 (2007).

29. Husseiny MI, El-Aziz MA, Badr Y, Mahmoud MA. Biosynthesis of gold nanoparticles using *Pseudomonas aeruginosa. Spectrochim Acta Part*

A **67**, 1003-1006 (2007).

30. Han JW, Gurunathan S, Jeong JK, Choi YJ, Kwon DN, Park JK, et al. Oxidative stress mediated cytotoxicity of biologically synthesized silver nanoparticles in human lung epithelial adenocarcinoma cell line. *Nanosci Res Lett* **9**,459 (2014). doi: 10.1186/1556-276X-9-459.

31. Tran QH, Nguyen VQ, Le AT. Silver nanoparticles: synthesis, properties, toxicology, applications and perspectives. Advnced in Natural Science: Nanoscience and Nanotechnology 4, 033001 (2013) doi.org/10.1088/2043-6262/4/3/03300.

32. Ahamed M, Alsalhi MS, Siddiqui MK. Silver nanoparticle applications and human health. *Clin Chim Acta* **411**, 1841-8 (2010).

33. Rahman M, Wang J, Patterson T, Saini U, Robinson B, Newport G, et al. Expression of genes related to oxidative stress in the mouse brain after exposure to silver-25 nanoparticles. *Toxicol Lett.* **187** (1),15-21(2009).

34. Sokołowska P, Bia łkowska K, Siatkowska M, Rosowski M, Kucińska M, Komorowski P, et al. Human brain endothelial barrier cells are distinctly Less vulnerable to silver nanoparticles toxicity than human blood vessel cells: A cell specific mechanism of the brain barrier? *Nanomed* **7**, 2127-2130 (2017).

35. Takenaka S, Karg E, Roth C, Schulz H, Ziesenis A, Heinzmann U, et al. Pulmonary and systemic distribution of inhaled ultrafine silver particles in rats. *Environ. Health Perspect.* **109** (Suppl. 4), 547 (2001).

36. Tang J, Xiong L, Wang S, Wang J, Liu L, Li J, et al. Distribution, translocation and accumulation of silver nanoparticles in rats. *J Toxicol Sci.* **9** (8), 4924-4932(2009).

37. Awasthi KK, Awasthi A, Kumar N, Roy A, Awasthi K, John P. Silver nanoparticles induced cytotoxicity, oxidative stress, and DNA damage in CHO cells. *J Nanoparticle Res.* **15** (9), 1898(2013) DOI 10.1007/s11051-013-1898-5.

38. Gopinath P, Gogoi SK, Sanpui P, Paul A, Chattopadhyay A, Ghosh SS. Signaling gene cascade in silver nanoparticle induced apoptosis, *Colloids Surf B: Biointerfaces* **77** (2), 240-245 (2010).

39. Abdel-Aziz MS, Shaheen MS, El-Nekeety AA**,** Abdel-Wahhab MA. Antioxidant and antibacterial activity of silver nanoparticles biosynthesized using *Chenopodium murale* leaf extrat. *J Saudi Chem Soc.* **18**, 356-363.

40. Parashar V, Parashar R, Pandey AC. Parthenium leaf extract mediated synthesis of silver nanoparticles: a novel approach for weed utilization. *Dig J Nanomater Bio* **4**, 45-50 (2009).

41. Leela A, Vivekanandan M. Tapping the unexploited plant resources for the synthesis of silver nanoparticles. *Afr J Biotechnol* **7**, 3162-3165 (2008).

42. Elavazhagan T, Arunachalam KD. *Memecylon edule* leaf extract mediated green synthesis of silver and gold nanoparticles. I*nt J Nanomed.* **6**, 1265-1278 (2011).

43. Kim DO, Jeong SW, Lee CY. Antioxidant capacity of phenolics phytochemicals from various cultivars of plums. *Food Chem.* **81**(3), 321-326 (2003).

44. Singh RP, Murthy KNC, Jayaprakasha GK. Studies on the antioxidant activity of pomegranate (*Punica granatum*) peel and seed extracts using *in vitro* models. *J Agric Food Chem.* **50**, 81-86 (2002).

45. Braca A, De Tommasi N, Di Bari L, Pizza C, Polit, M, Morelli I. Antioxidant principles from *Bauhinia terapotensis*. *J Nat Prod.* **64**,892-895(2001).

46. Wettasinghe M, Shahidi IF. Evening primrose meal: a source of natural antioxidants and scavenger of hydrogen peroxide and oxygen-derived free radicals. *J Agric Food Chem.* **47** (5), 1801-1812(1999).

47. Henry RJ. Clinical chemistry, principles and technics. Harper & Row. New York. P. 644-646 (1974).

48. Smith, AJ. A colorimetric method for the estimation of serum magnesium. *Biochem J.* **60**(3), 522-7 (1955).

49. Lin CC, Hsu YF, Lin TC, Hsu FL, Hsu HY. Antioxidant and hepatoprotective activity of punicalagin and punicalin on carbon tetrachloride induced liver damage in rats. *J Pharmacol.* **50**, 789-794(1998).

50. Drury RA, Wallington EA. Carleton's Histological Technique. 5th Edition, Oxford University Press, New York (1980).

51. Thakur P, Sanyal SN. Chemopreventive role of preferential COX-2 inhibitor diclofenac in 9, 10-Dimethybenz(a)anthracene induced experimental lung carcinogenesis. *Amer J Biomed Sci.* **2**(3), 275-288 (2010).

52. Abdel-Wahhab MA, El-Nekeety AA, Salman AS, Abdel-Aziem SH, Mehaya FM, Hassan NS. Protective capabilities of silymarin and inulin nanoparticles against hepatic oxidative stress, genotoxicity and cytotoxicity of Deoxynivalenol in rats. *Toxicon* **142**, 1-13)2018)

53. Raben N, Nichols RC, Martiniuk F, Plotz PH. A model of mRNA splicing in adult lysosomal storage disease glycogenosis type II. *Human Mol Genet.* **5**, 995-1001(1996).

54. SAS institute, Inc SAS Users Guide: Statistics. SAS Institute, Cary, NC. (1982).

55. Waller RA, Duncan DB. A Bayes rule for the symmetric multiple comparison problems. *J Am Stat Assoc.* **64**, 1484-1503(1969).

56. Saxena A, Tripathi RM, Singh RP. Biological synthesis of silver nanoparticles by using onion (*Allium cepa*) extract and their antibacterial activity. *Dig J Nanomater Bio.* **5**, 427-432(2010).

57. Awika JM, Rooney LW, Wu X, Prior RL, Zevallos LC. Screening methods to measure antioxidant activity of sorghum (*Sorghum bicolor*) and sorghum products. *J Agric Food Chem.* **51**, 6657-6662(2003).

58. Chang ST, Wu JH, Wang SY, Kang PL, Yang NS, Shyur LF. Antioxidant activity of extracts from Acacia confusa bark and heartwood. *J Agric Food Chem.* **49**, 3420-3424(2001).

59. Laghari A, Memon S, Nelofar A, Khan MK, Yasmin A. Determination of free phenolic acids and antioxidant activity of methanolic extracts obtained from fruits and leaves of *Chenopodium album*. *Food Chem.* **126**, 1850-1855(2011).

60. Emam SS. Bioactive constituents of *Atriplex halimus* plant. *J Nat Prod.* **4**, 25-41(2011).

61. Nsimba RY, Kikuzaki H, Konishi Y. Antioxidant activity of various extracts and fractions of *Chenopodium quinoa* and *Amaranthus* spp. seeds. *Food Chem.* **106**(2), 760-766 (2008).

62. Sung JH, Ji JH, Park JD, Yoon JU, Kim DS, Jeon KS et al. Subchronic inhalation toxicity of silver nanoparticles. *Toxicolo Sci.* **108**, 452-461(2008).

63. Abdel-Wahhab MA, Aljawish A, El-Nekeety AA, Abdel-Aziem SH, Abdel-Kader HAM, Rihn BH et al. Chitosan nanoparticles and quercetin modulate gene expression and prevent the genotoxicity of aflatoxin B_1 in rat liver. *Toxicol Rep.* **2**, 737-747(2015).

64. Adeyemi OS, Uloko RA, Awakan OJ, Adeyanju AA, Otohinoyi DA. The oral administration of silver nanoparticles activates the kynurenine pathway in rat brain independently of oxidative stress. *Chem-Biol Interact.* **302**, 22-27 (2019).

65. Fernández MN, Muñoz-Olivas R, Luque-Garcia JL. SILAC-based quantitative proteomics identifies size-dependent molecular mechanisms involved in silver nanoparticles-induced toxicity. *Nanotoxicol.* **18**, 1-15 (2019).

66. Tang J, Lu X, Chen B, Cai E, Liu W, Jiang J et al. Mechanisms of silver nanoparticles-induced cytotoxicity and apoptosis in rat tracheal epithelial cells. *J Toxicol Sci.* **44**(3), 155-165 (2019).

67. Nam SH, An YJ. Size- and shape-dependent toxicity of silver nanomaterials in green alga *Chlorococcum infusionum*. *Ecotoxicol Environ Saf.* **168**, 388-393 (2019).

68. El Mahdy MM, Eldin TA, Aly HS, Mohammed FF, Shaalan MI. Evaluation of hepatotoxic and genotoxic potential of silver nanoparticles in albino rats. *Exp Toxicol Pathol.* **67**(1), 21-29(2014).

69. Ryter SW, Kim HP, Hoetzel A, Park JW, Nakahira K, Wang X, et al. Mechanisms of cell death in oxidative stress. *Antioxid Redox Sign.* **9**, 49-89 (2007).

70. Kim YS, Song MY, Park JD, Song KS, Ryu HR, Chang HK, et al. Subchronic oral toxicity of silver nanoparticles. *Part Fiber Toxicol.* **7**(1), 20 (2010) doi: 10.1186/1743-8977-7-20.

71. Song XL, Li B, Xu K, Liu J, Ju W, Wang J, et al. Cytotoxicity of water soluble mPEG-SH-coated silver nanoparticles in HL-7702 cells. *Cell Biol Toxicol.* **28**(4), 225-237(2011).

72. Mei N, Zhang Y, Chen Y, Guo X, Ding W, Ali, S. et al. Silver nanoparticle-induced mutations and oxidative stress in mouse lymphoma cells. *Environ Mol Mutagen.* **53**, 409-19(2012).

73. Ghosh MJM, Sinha S, Chakraborty A, Mallick SK, Bandyopadhyay M, Mukherjee A. *In-vitro* and *in-vivo* genotoxicity of silver nanoparticles. *Mutat Res.* **18**, 00274-4 (2012).

74. Stensberg MC, Wei Q, McLamore ES, Porterfield DM, Wei A, Sepúlveda MS. Toxicological studies on silver nanoparticles: challenges and opportunities in assessment, monitoring and imaging. *Nanomedicine* (Lond) **6**, 879-98(2011).

75. Singh RP, Ramarao P. Cellular uptake,

intracellular trafficking and cytotoxicity of silver nanoparticles. *Toxicol Lett.* **213**, 249-259(2012).

76. Ansari MA, Khan HM, Khan AA, Alzohairy MA, Waseem M, Ahmad MK, et al. Biochemical, histopathological, and transmission electron microscopic ultrastructural changes in mice after exposure to silver nanoparticles. *Environ Toxicol.* **31**(8), 945-956(2016).

77. Korani M, Rezayat SM, Bidgoli SA. Sub-chronic dermal toxicity of silver nanoparticles in Guinea pig: special emphasis to heart, bone and kidney toxicities. *Iran J Pharm Res.* **12** (3), 511-519(2013).

78. Sardari RRR, Zarchi SR, Talebi A, Nasri S, Imani S, Khoradmehr A, et al. Toxicological effects of silver nanoparticles in rats. *Afr J Microbiol Res* **6**(27), 5587-5593(2012).

79. Tiwari R, Singh RD, Khan H, Gangopadhyay S, Mittal S. Oral subchronic exposure to silver nanoparticles causes renal damage through apoptotic impairment and necrotic cell death. *Nanotoxicol*. **11**(5), 671-686 (2017).

80. Vasanth SB, Kurian GA. Toxicity evaluation of silver nanoparticles synthesized by chemical and green route in different experimental models. *Artif Cells Nanomed Biotechnol.* **45**(8), 1721-1727 (2017).

81. Heydrnejad MS, Samani RJ. Sex differential influence of acute orally-administered silver nanoparticles (Ag-NPs) on some biochemical parameters in kidney of mice *Mus musculus*. *J Nanomed Nanotechnol.* **7**, 382(2016). doi:10.4172/2157-7439.1000382.

82. Adeyemi OS, Adewumi I, Faniyan TO. Silver nanoparticles influenced rat serum metabolites and tissue morphology. *J Basic Clin Physiol Pharmacol.* **26**, 355-361 (2015).

83. Ji JH, Jung JH, Kim SS, Yoon JU, Park JD, Choi BS, et al. Twenty-eight-day inhalation toxicity study of silver nanoparticles in Sprague-Dawley rats. *Inhal Toxicol*. **19**, 857-871 (2007).

84. Kvitek L, Vanickova M, Panacek A. Initial study on the toxicity of silver nanoparticles (NPs) against *Paramecium caudatum*. *J Phys Chem C.* **113**, 4296-4300 (2009).

85. Ravi V, Saleem TSM, Patel SS, Raamamurthy J, Gauthaman K. Anti-Inflammatory effect of methanolic extract of *Solanum nigrum* Linn berries. *Int J Appl Res Nat Prod*. **2(2)**, 33-36 (2009)**.**

86. Lin HM, Tseng HC, Wang CJ, Lin JJ, Lo CW, Chou FP. Hepatoprotective effects of *Solanum nigrum* Linn extract against CCl_4-induced oxidative damage in rats. *Chem Biol Interact*. **171**(3), 283-93(2008).

87. Gawlik-Dziki U, Świeca M, Sułkowski M, Dziki D, Baraniak B, Czyż J. Antioxidant and anticancer activities of *Chenopodium quinoa* leaves extracts - *in vitro* study. *Food Chem Toxicol.* **57**, 154-160(2013).

88. Kukrića ZZ, Topalić-Trivunović LN, Kukavica BM, Matoš SB, Pavičić S, Boroja MM, et al. Charaterization of antioxidant and antimicrobial activities of nettle leaves (*Urtica dioica* L.). BIBLID **43**, 257-271(2012).

89. Kumar R, Kumar D, Patwa R. Evaluation of phytochemical constituents and antioxidant activity of *Chenopodium album* of Bundelkhand region. *J Pharm Res.* **12**(1), 81-86(2018).

90. Samanta P, De, S. Study on the antibacterial, antioxidant activities and phytochemical analysis of medicinal plants in West-Bengal. Inter *JCurr Microbiol Appl Sci.* **4**(10), 116-123(2015).

91. Nagalekshmi R, Menon A, Chandrasekaran DK, Nair CK. Hepatoprotective activity of *Andrographis paniculata* and *Swertia chirayita. Food Chem. Toxicol.* **49** (12), 3367-3373(2011).

92. Van Der Hoeven JAB, Moshage H, Schuurs T, Nijboer M, Van Schilfgaarde R, Ploeg RJ. Brain death induces apoptosis in donor liver of rat. *Transplantion* **76**(6), 1150-1154 (2003).

93. Kurtulus A, Dodurga Y, Yonguc GN, Sorkun HC, Boz B, Kemalettin AK. Effect of short-term exposure to dichlorvos on rat hepatocyte: molecular and histopathological approach. *Rom J Leg Med*. **20**,155-160 (2012).

94. Wiame I, Remy S, Swennen R, Sági L. 2000. Irreversible heat inactivation of DNaseI without RNA degradation. *Biotechniques* **29**, 252-256(2000).

الزيت العطري لنبات الرمرام يخفف من السمية الوراثية والكرب التأكسدي الناتج عن جسيمات الفضة النانونية في كلية الفئران

مسعد عطية عبد الوهاب[١]، حلمي معوض سيد احمد[٢]، عزيزة عبد السلام النقيطي[١]، سكينة حسانين عبد العظيم[٣]، حفيظه عبد السميع شرف[٤]، محمد سيد عبد العزيز[٥]، محمد فتحي سلام[٦]، فتحية عبد الواحد مناع[٧]

[١]قسم سموم وملوثات الغذاء- المركز القومي للبحوث- الدقي- مصر.

[٢]قسم الأدوية والسموم- كلية الصيدلة- جامعة القاهرة- القاهرة- مصر.

[٣]قسم الوراثة الخلوية- المركز القومي للبحوث- الدقي- مصر.

[٤]قسم الباثولوجيا الطبية- المركز القومي للبحوث- الدقي- مصر.

[٥]قسم كيمياء الكائنات الدقيقة- المركز القومي للبحوث- الدقي- مصر.

[٦]مستشفى قصر العيني الجديد- القاهرة- مصر.

[٧]قسم الفسيولوجيا الطبية- المركز القومي للبحوث- الدقي- مصر.

استهدفت هذه الدراسة بناء جسيمات فضة نانونية باستخدام مستخلص نبات الرمرام ثم تقييم النشاط المضاد للأكسدة والدور الوقائي للزيت العطري للنبات ضد تسمم الكلى الناتج عن جسيمات الفضة النانونية في الفئران. استخدمت في هذه التجربة إناث فئران سبرغ داولي حيث قسمت الى سبع مجموعات تم معاملتها عن طريق الفم لمدة ٢١ يوما وشملت المجموعة الضابطة، المجموعات المعاملة بجسيمات الفضة النانونية بجرعات ٢٥ او ٥٠ ملجم / كجم من وزن الجسم، المجموعات المعاملة بزيت نبات الرمرام بجرعات ٠,٥ أو ١ ملجم/ كجم من وزن الجسم والمجموعات المعاملة بجسيمات الفضة النانونية مع الزيت بنفس الجرعات السابقة. أثبتت النتائج ان حجم جسيمات الفضة المتكونة يتراوح بين ٣٠-٥٠ نانوميتر. أوضحت النتائج ايضا أن زيت نبات الرمرام غني بالفينولات الكلية والفلافونيدات وأظهر نشاطا مضاد للأكسدة وقدرة عالية على كسح الجذور الحرة معمليا. كما أوضحت النتائج ايضا أن جسيمات الفضة النانونية احدثت اضطرابا في وظائف الكلى ، وانخفاض الإنزيمات المضادة للأكسدة ، وزيادة الجذورالحرة في المصل وعامل النخر الورمي وتأكسد الدهون واكسيد النتريك وزيادة تعبير جين البروتين من النمط ٢-*Bcl*، TNF-α بينما ادت إلى نفص تعبير جينات Bax و P*53* بالاضافة إلى حدوث تغيرات باثولوجية في انسجة الكلية. هذا وقد أثبتت النتائج قدرة الزيت العطري لنبات الرمرام على حماية الكلية من التغيرات المرضية الناتجة عن التعرض لجسيمات الفضة النانونية كما أن هذه الجماية كانت تتناسب مع الجرعة المستخدمة من الزيت. نستخلص من هذه الدراسة أن التعرض لجسيمات الفضة النانونية يسبب تسمم للكلي وزيادة الجذور الحرة ونقص مضادات الاكسدة مما ينتج عنه حالة من الكرب التأكسدي بالجسم كما أن الزيت العطري لنبات الرمرام له قدرة فائقة على معالجة هذه الاثار السامة ويمكن اعتباره مكملا غذائيا للفئات الاكثر تعرضا لجسيمات الفضة النانونية.